C.E.D. Riboldi, L. Trainelli, F. Biondani
Structural Batteries in Aviation: a Preliminary Sizing Methodology
Journal of Aerospace Engineering, Vol. 33, N. 4, 2020, 04020031 (15 pages)
doi:10.1061/(ASCE)AS.1943-5525.0001144

STRUCTURAL BATTERIES IN AVIATION: A PRELIMINARY SIZING METHODOLOGY

Carlo E.D. Riboldi[1],

Lorenzo Trainelli[1],

and Fabio Biondani[1]

ABSTRACT

A significant research effort in aviation is currently focused on the integration of electric or hybrid-electric power-trains on board aircraft in an effort to improve efficiency and environmental friendliness. New designs incorporating these novel propulsion systems face the issue of penalizing battery characteristics, especially in terms of limited energy and power density performance, in turn imposing a toll on the inert weight of the machine. A possible solution to this issue is that of structural batteries. These are similar in structure to carbon fiber composites, where the matrix features dielectric characteristics, making the structure capable of storing electric energy while retaining the capability to withstand mechanical loads. The adoption of this technology, currently under advanced development, shall enable significant weight savings, yet it raises relevant issues concerning aircraft sizing procedures, that need to be conceived taking into account the specific characteristics of such multi-functional materials. This paper faces the new problem of aircraft initial design in presence of structural batteries. First, it presents a method for aircraft preliminary weight sizing, where the double effect of structural batteries on both structural mass and energy storage mass is considered. Subsequently, a procedure to size an airframe structure with the adoption of structural batteries in key components is shown, based on a weight-optimal approach. The complete sizing procedure is illustrated through an award-winning test case in the General Aviation category.

Keywords: structural batteries, multi-functional material, electric aircraft, hybrid-electric propulsion, aircraft design, preliminary sizing

INTRODUCTION

All-electric and hybrid-electric propulsion for aircraft represent promising alternatives to conventional internal combustion engines (ICE), especially for light General Aviation (GA) aircraft. This is thanks to the lower noise and polluting emissions granted by the electric component of the power-train, which allows

[1]Dept. of Aerospace Science and Technology, Politecnico di Milano, via La Masa 34 - 20156 Milano, Italy. E-mail: carlo.riboldi@polimi.it

to mitigate acceptance issues by communities in the vicinity of local airports and to increase comfort on board (Cohen and Coughlin 2008; Morrell and Lu 2000).

As of today, some all-electric aircraft have been designed and flown (see (Riboldi and Gualdoni 2016) for a list of models). Most of them are basically electrified versions of existing gliders, like the Lange Aviation Antares 20E and 23E (Lange Aviation GmbH), or the Pipistrel Taurus Electro G2 (Pipistrel Vertical Solutions d.o.o.). Others are very light machines, inspired from a corresponding conventionally-powered aircraft in the Light Sport Aircraft (LSA) category. Among them can be found the Yuneec International E430 (Yuneec Americas (USA)) or the Pipistrel Alpha Electro (Pipistrel Vertical Solutions d.o.o.). The very low weight and high lift-to-drag characteristics of these models is strongly related to the significant weight toll inherent to all-electric aircraft. In the field of hybrid-electric propulsion, even less specimens exist, and currently there is not a single hybrid-electric aircraft available on the market. However, today research is particularly active in that field (Bona et al. 2014; Friedrich and Robertson 2015), with many design proposals of which only a few have been actually manufactured and tested. The most recent are the Diamond DA-36 E-Star (Diamond Aircraft Industries GmbH) in Europe and the Ampaire 337 (Ampaire Inc.) in the USA.

Most recently, the EU has been fueling interest in hybrid-electric propulsion through project MAHEPA, which among its expected outcomes includes the production and testing of a serial hybrid-electric GA aircraft, the study of dedicated, scalable aircraft design techniques capable of handling larger weight categories, and an analytic forecast of the presumed impact of hybrid-electric propulsion on the air transport market in the near future (Trainelli and Perkon 2019). This effort resulted in the development of general preliminary sizing methodologies for all-electric and hybrid-electric airplanes (Rossi et al. 2018; Trainelli et al. 2019b), including the case of hydrogen fuel-cell driven aircraft (Trainelli et al. 2019a).

Currently, one of the major obstacles to the quick growth of these propulsion technologies is the limited performance of batteries. In particular, their low weight-specific power and energy storage capabilities impose a relevant toll on the overall weight of the aircraft, in spite of a moderate contribution to the energy amount stored for propulsion (Cao et al. 2012; Hagen et al. 2013; Hagen et al. 2015). By comparison, normal hydrocarbon (HC) fuel provides energy density figures which are typically higher than for batteries by a ratio 12:1, for most high-performing research batteries, to more than 60:1, for standard Lithium-ion batteries (Ozawa 2009). Furthermore, batteries usually result in bulky components, possibly difficult to allocate on board.

An interesting technology, with the potential to boost electric energy storage capabilities of aircraft, is constituted by structural batteries (SB) (Asp and Greenhalgh 2014; Gienger et al. 2015; Adam et al. 2018). These are multi-functional structural components, manufactured similarly to composite materials already used on many aircraft, and capable of replacing stress-supporting parts typically made from metal alloys or carbon-fibers. Besides good load-bearing characteristics, structural batteries can store electrical energy. Components made of SB can be molded to assume curvatures compatible with the requirements of aircraft lofting, especially on the fuselage and wing panels, just as with typical composite materials. The adoption of this material for designing an all-electric or hybrid-electric aircraft allows savings on both the weight of conventional batteries and on structural weight, thus providing a double advantage with respect to the adoption of conventional singly-functional materials.

The present paper deals with the brand-new problem of initial design of an aircraft using SB in key components. This involves both preliminary sizing in a conceptual design phase and airframe structural sizing in support to preliminary design activities. At first, a procedure for including structural batteries in the loop of preliminary sizing of a serial hybrid-electric light GA aircraft is described, showing a way to face the peculiar effect of the presence of SB on the computation of design component weights, the values of which are all inherently coupled given the effect of SB on airframe structural weight and energy-related weight. The desired performance of the aircraft is rigorously taken into account, and the results of the presented procedure are the weights of both conventional and structural batteries, and all the other components of the design take-off weight. Subsequently, the paper outlines a procedure for the sizing of the most stressed sections on the structural components of a typical GA aircraft, based on a weight-optimal approach. Together, these two methodologies provide a comprehensive procedure to carry out the structural design of a GA aircraft with SB. The procedure is then demonstrated through the example of the award-winning project of a GA aircraft named *Hybris*, showing also excerpts of the sizing of the overall structural layout (Bernasconi et al. 2017).

STRUCTURAL BATTERY TECHNOLOGY

The technology of SB is based on the exploitation of the structural characteristics of laminated electrodes, stacked in a sandwich with an electrolyte layer between them, as sketched in Figure 1.

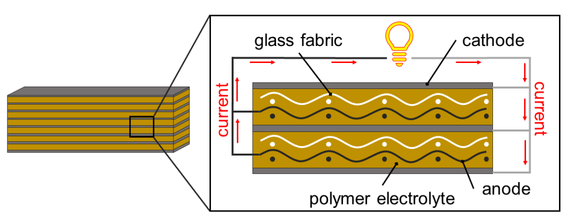

FIG. 1. Structural battery technology concept.

The first published works on the matter investigated the use of laminated electrodes with a share of

Year	Energy Density
2010	116 Wh/kg
2014	175 Wh/kg
2015	200 Wh/kg

TABLE 1. Time evolution of energy density for structural batteries.

carbon fibers, and liquid or gel electrolytes. These batteries resulted incapable of simultaneously sustaining significant structural loads and providing for a relevant electric energy storage capability (Wong et al. 2007; Liu et al. 2009).

A more promising technological approach features carbon fibers electrodes joined through a mainly porous matrix, chemically and micro-structurally designed to sustain loads. The porous matrix is filled in the manufacturing process with a resin material with good electrolyte properties (Snyder et al. 2007; Wetzel 2010). This technique is the result of an extensive experimental analysis, where different materials have been tried to create a binding layer between the carbon fiber electrodes, yielding acceptable multi-functional properties (Gienger et al. 2015).

Table 1 reports results from the existing literature, highlighting the positive trend in terms of energy density, *i.e.* stored energy per unit mass, for multi-functional battery technology (Asp and Greenhalgh 2014; Ekstedt et al. 2010; Asp 2013). In the present work, these figures have been extrapolated to the present day, and a 0.5 safety margin has been adopted for further computations, in consideration of the experimental nature of the database, as shown in a later section. This approach yields the energy and power features of structural batteries presented in Table 2.

Table 2 and 3 present achievable properties for SB at the current level of technology. In Table 2, e_b represents energy density, $p_\text{b-peak}$ and p_b peak and continuous power density, *i.e.* power output per unit mass, respectively. From Table 3, where SB characteristics are contrasted to those of Carbon Fiber Reinforced Polymer (CFRP) composites, it is seen that many mechanical properties are comparable, with the exceptions of compression and shear strenghts, two important items that shall lead to specific choices in the structural architecture in the following. Also, in terms of mass density, SB are in a range comparable with Lithium-ion batteries (typically 1.5 to 2.8 g/cm^3 (Pearson et al. 2004)), but their multi-functional features make them advantageous also in this respect.

These values are in line with the results of the experiments on structural batteries with a binder made of a monolith filler enriched with an electrolyte resin (Snyder et al. 2016). These properties have been assumed also in the production of the results presented in this paper. They reflect a conservative approach, where the

Battery type	Conventional	Structural
e_{b} [Wh/kg]	265	125
$p_{\text{b-peak}}$ [W/kg]	2 600	1 200
p_{b} [W/kg]	900	400

TABLE 2. Design battery energy and power densities.

Quantity	CFRP	SB
Mass density [kg/m^3]	1 600	1 800
Tensile modulus [GPa]	70	70
Shear modulus [GPa]	5.2	5.0
Ultimate tensile strength 0° [MPa]	600	560
Ultimate compression strength 0° [MPa]	570	280
Ultimate tensile strength 90° [MPa]	600	560
Ultimate compression strength 90° [MPa]	570	280
Ultimate in-plane shear strength [MPa]	90	52
Ply thickness [mm]	0.20	0.275

TABLE 3. Structural features of the considered composite materials.

material is basically performing worse than both a conventional battery and a typical structural composite. This was deemed necessary due to the immaturity of this technology and the proposed application to the new field of aviation.

Nevertheless, it will be shown in the results that, even with these penalizing assumptions, the use of SB appears very promising for aeronautical applications. It is likely that, due to the ongoing research in the field of SB (Adam et al. 2018; Johannisson et al. 2018; Carlstedt et al. 2019), the precautionary results presented herein will be significantly improved in the near future.

AIRCRAFT PRELIMINARY SIZING

While the general feasibility of an aircraft design has been already investigated (Scholz et al. 2018), the in-depth structure of a possible design procedure has not been consolidated yet. The adoption of SB poses relevant issues to aircraft designers, for the integration of this material in a novel aircraft calls for sizing procedures specifically accounting for their multi-functional properties. In particular, SB are both part of the structural weight and of the empty energy storage weight, resulting in a failure of the classical definition of gross weight break-down (Raymer 2012).

Therefore, the preliminary sizing of an airplane using SB needs a tailored procedure, detailed hereafter and based on the following gross weight break-down:

$$W_{\text{to}} = W_{\text{cs}} + W_{\text{ns}} + W_{\text{sb}} + W_{\text{cb}} + W_{\text{f}} + W_{\text{pl}}, \tag{1}$$

where W_{cs} stands for the structural weight from conventional materials, W_{ns} for the non structural part of the empty weight (including the propulsion system), W_{sb} for the structural weight from SB, W_{cb} for the weight of conventional batteries, W_{f} for the fuel weight, and W_{pl} for the payload weight, respectively.

At present, we shall focus on a serial hybrid-electric propulsive architecture, *i.e.* the case in which the thermal (ICE) component in the power-train acts only as an electric power generation system, without contributing to the mechanical power delivered to the propeller, which is provided by the EM. This architecture is sketched in Figure 2.

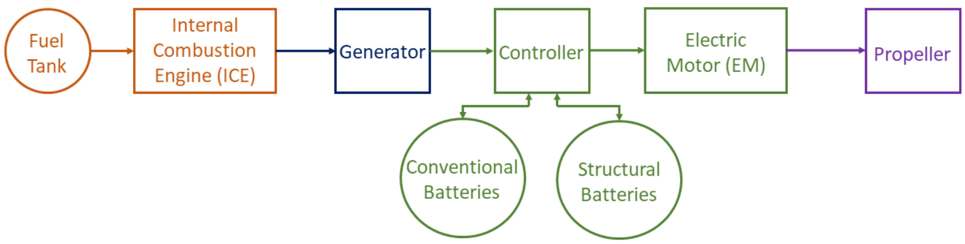

FIG. 2. Serial hybrid-electric architecture with conventional and structural batteries.

The loop for the preliminary sizing of a serial-hybrid aircraft with SB is shown in Figure 3. The procedure is based on some assumptions, and on the specification of the performance requirements. The blocks of the flowchart will be presented in detail in the following subsections.

Initialization

In the design of a new aircraft, the preliminary sizing loop is usually launched following an analysis of the target market, which helps in the negotiation of some desired specifications and in the definition of the characteristics of the aircraft configuration – e.g. number of engines, wing positioning, undercarriage type, tail configuration – as well as a certification basis.

With respect to the procedure presented herein, such a phase would help providing an estimate of some basic qualities of the aircraft, bound to its configuration. Firstly, estimates of the polar curves of the aircraft need to be provided. A usual model where $C_D = C_{D_0} + \frac{1}{\pi \lambda e} C_L^2$ can be adopted, where C_D stands for the aircraft drag coefficient and C_L for the lift coefficient. The characteristic coefficients to be assigned are the aspect ratio λ, Oswald coefficient e and parasite drag coefficient C_{D_0}. These should be guessed somehow, for instance through the methods proposed by Roskam (Roskam 2003) for different aircraft configurations. Such methods allow to take into account also changes in the aerodynamic characteristics due to configuration changes from clean to take-off or landing, without the need to accurately size the high-lift surfaces, and

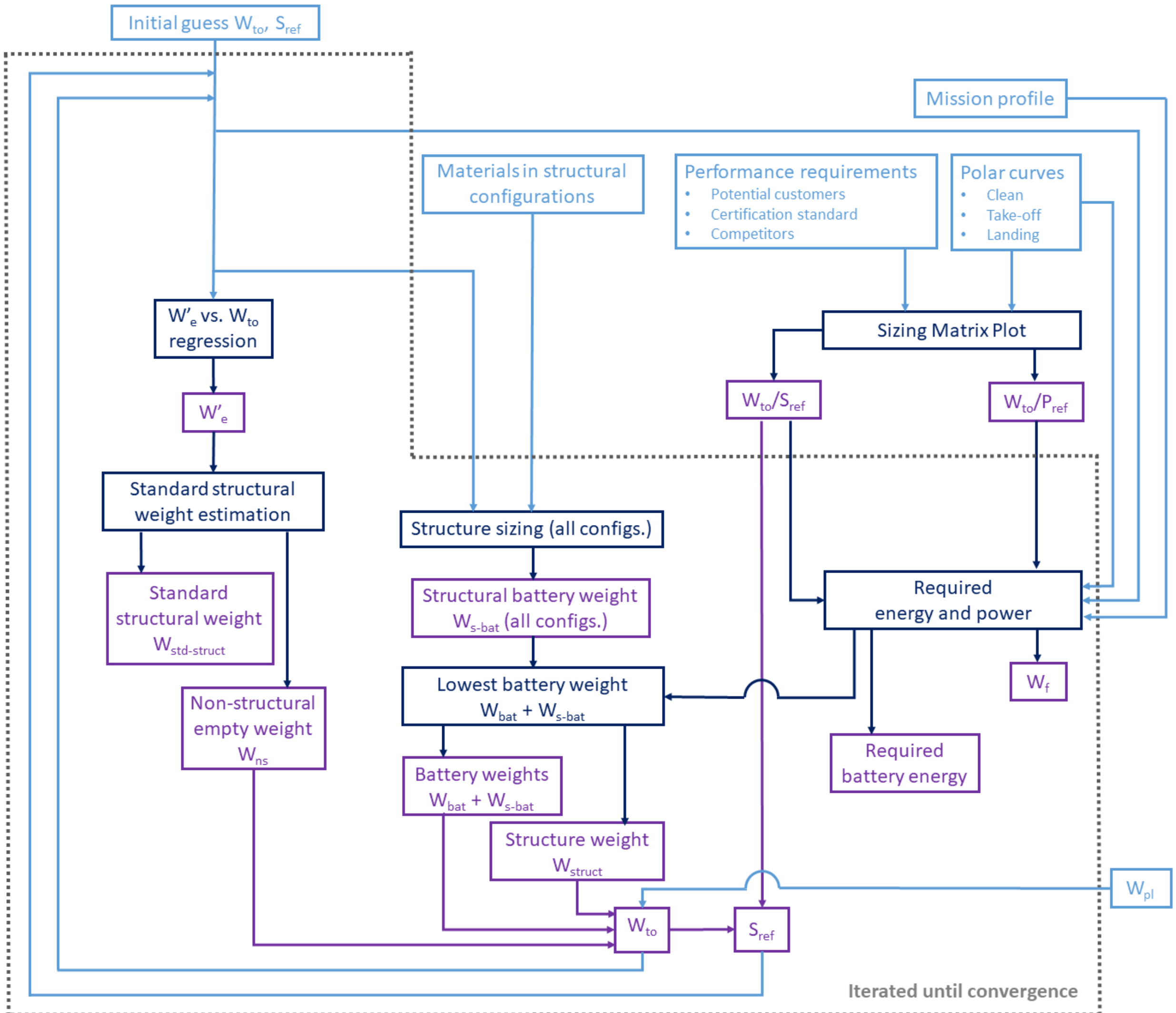

FIG. 3. Preliminary aircraft weight sizing flowchart.

considering the landing gear being either retractable or fixed. An estimate of the maximum lift coefficient $C_{L,\max}$ should be provided too. The adoption of SB in the design does not affect the aerodynamic shape of the aircraft, for this material can be molded similarly to single-functional composites in curved shapes. Therefore, rather standard techniques for preliminary aerodynamic analysis can be safely used.

A second major element needed to initialize the sizing procedure is the sizing matrix plot (SMP), also indicated as matching plot, corresponding to assigned performance requirements (Raymer 2012). The SMP allows merging the requirements generated by the desired performance of the aircraft and those emerging from certification rules. In order to set up this analysis, it is necessary to figure out the characteristics of the flight profile of the sizing mission(s), which in turn is part of the characterization of the design scenario of interest.

For a propeller-driven aircraft, each requirement is translated into a curve on a power loading $W_{\mathrm{to}}/P_{\mathrm{b}}$ vs. wing loading $W_{\mathrm{to}}/S_{\mathrm{ref}}$ plane, where W_{to} stands for design take-off weight, P_{b} for installed (brake) power, and S_{ref} for the aircraft reference surface, which is typically the area of the wing planform. Usually, requirements from desired performance or certification specifications include limitations on the stall speed, maximum take-off distance and landing distance, minimum climb rate, and a cruise and loiter speed performance. These are basic requirements typically appearing in the design of LSA and GA. Clearly, other requirements may appear considering different design cases, specific to the mission the aircraft is intended to fly. Their corresponding curves should be considered on the SMP as well. The analysis of the SMP allows to draw the space of solutions in the considered domain. The curves on the SMP will be quantitatively bound to the assumed aerodynamic polar curves of the aircraft. By selecting a point in that space, the design values for the ratios $W_{\mathrm{to}}/P_{\mathrm{b}}$ vs. $W_{\mathrm{to}}/S_{\mathrm{ref}}$ will be set automatically in such a way to comply with all considered requirements.

The choice of the design point in the space of solutions on the SMP may vary according to the adopted design strategy. A typical guideline consists in reducing the necessary power as much as possible, hence choosing the maximum attainable $W_{\mathrm{to}}/P_{\mathrm{b}}$, while also reducing the size of the aircraft through a lower S_{ref}, by selecting the maximum $W_{\mathrm{to}}/S_{\mathrm{ref}}$. On the other hand, the wing may be an area where SB can be profitably placed, making it particularly attractive to increase the storage of electric energy on board. For this reason the choice of the design point on the SMP may be the result of a trade-off, considering in particular the presence of the new battery technology. The analysis of the SMP is highlighted in a dedicated block of Figure 3.

Being structured as an iterative process, the design loop starts from an initial guess of the take-off weight W_{to} and of the reference wing area S_{ref}, as specified in Figure 3.

Mission power and energy requirements

In order to compute the energy necessary to a given flight profile, the basic characteristics of the mission need to be known. The typical flight profile for a LSA or GA usually includes five phases: take-off, climb, cruise, loiter, and landing. Energy quotas can be defined corresponding to each of these phases based on basic flight mechanics equilibrium considerations. For a sport or training aircraft, the large majority of the energy on board is needed to cover the climb, cruise and loiter phases (Riboldi and Gualdoni 2016; Riboldi et al. 2018; Riboldi 2018). For a hybrid-electric aircraft, the energy to be stored on board as HC fuel and in batteries, respectively, has to be determined based on the energy management strategy for the flight profile.

It should be noted that, as the present paper is not centered on the topic of designing a power management system, the presented procedure does not consider the characteristics of the energy management strategy as design parameters to be tuned, but assumes a specified strategy defined from the start and kept constant during the iterations. A more complex approach, including optimal energy management determination, may be developed along the lines presented in (Riboldi 2018; Rossi et al. 2018; Trainelli et al. 2019b)

To provide a quick example of the effect of the choice of a power management strategy on the computations of interest here, it suffices to remember that for a serial-hybrid the ICE is used to provide electric power, which supplies an EM used for propulsion. Therefore, a larger amount of HC fuel would ensure a generally longer range and endurance, whereas a larger amount of batteries would provide a similar increase in flight performance, without the need to switch on the ICE. When public acceptance is at a premium, as it is often the case for smaller aircraft operating from local airport in crowded areas, the ability to take-off and climb in fully electric mode – *i.e.* without the need to burn HC fuel – is of great interest. To this end, the amount of electric energy may be sized up to cover take-off and climb, at least to a transition altitude where the noise and chemical emissions produced by the ICE are no more a crucial issue. On the other hand, fuel tanks will be sized to allow powering the desired cruising and loiter phases, which are flown at higher altitudes, where again constraints on keeping the ICE running do not apply.

Once the flight profile and the corresponding energy management strategy have been determined, computations of the needed energy quotas can be carried out for all considered phases of flight (Riboldi and Gualdoni 2016; Riboldi et al. 2018; Riboldi 2018). All computations refer to an assigned value of W_{to} and S_{ref}, where the first is guessed and the second is computed from the first, based on the choice of the design point on the SMP.

It should be noted that this part of the procedure is used to size the needed energy amounts E_{f} and E_{e} of the fuel and batteries, respectively, as well as the required propulsive power, from which the needed electric power supply P_{e} can be obtained. Fuel weight can be computed from fuel energy, whereas the weight of the batteries needs to be split between structural and conventional batteries. Therefore, this energy analysis produces a quantitative definition of fuel weight W_{f} and electric energy E_{e} to be stored in the total battery pack.

Option ID	Use of SB	Use of CFRP
1	None	All components
2	Lower panels	Stringers, upper panels
3	Lower stringers, lower panels	Upper stringers, upper panels
4	Lower stringers, all panels	Upper stringers
5	All panels	All stringers
6	All stringers	All panels
7	All components	None

TABLE 4. Structural configuration alternatives for preliminary wing weight sizing.

Structural configuration

In order to determine the amount of SB to be stored on board, a selection procedure is proposed based on the analysis of some candidate structural configurations. In particular, while the use of SB in the fuselage does not raise particular issues bound to stress limits, due to their comparatively limited aerodynamic loading, the specific load resistance of SB is a primary matter of concern when it comes to place them in the wings.

Based on a straightforward hypothesis on the construction of the wing section, a series of wing structure options can be analyzed, where the share of SB over standard composite is progressively incremented. To this aim, a semi-monocoque construction can be typically adopted, arranged to constitute a close section. The wing can be preliminarily sized using a method proposed by Gudmundsson (Gudmundsson 2013), adjusted for this application. The method allows to estimate the size of the spar caps, the spar web and the thickness of the panels in a closed form. The relative chordwise extension of the structural section can be assigned with respect to the mean aerodynamic chord of the wing, which can be computed from the aspect ratio λ and current value of the wing reference surface S_{ref}.

Table 4 lists seven proposed options. It is possible to notice that the first option is a configuration where the wing is totally made of standard CFRP, whereas to the opposite in the last option considered where the whole wing structure is made of SB. Not all possible combinations have been taken into account. In particular, considering the limited performance of SB under compression forces, due to the poor mechanical properties of the matrix (Snyder et al. 2016), a configuration with the upper wing panels and stringers made with SB was not considered.

More in general, the limited properties under compression, as well as the need to replace the structural batteries when these approach the end of their lifetime, limits the adoption of SB in components like the upper panels and stringers in the wings, whereas the latter suggests the use of this material only in the most accessible parts of the aircraft.

Besides SB, CFRP composites can be considered for the rest of the structure, whereas steel can be used for junctions, representing only a residual component of the structural weight. The choice of this particular composites is reasonable due their adoption for the most recent designs in the GA field, in turn resulting from their good mechanical characteristics in spite of a slightly higher cost with respect to Glass Fiber Reinforced Polymers (Botelho et al. 2006). Furthermore, such higher cost is also expected to decrease over the years (Rao et al. 2015).

From a technological point of view, SB are assembled with alternate plies of carbon fibers coated in an electrolyte matrix and cathodic material, which ensure the desired energy storage capabilities (Asp and Greenhalgh 2014). Currently no SB has reached a sufficient maturity to be tested on-board. The assumption that the structural batteries could provide a compression and shear strength roughly half that of a composite material of similar thickness and power/energy density half that of a Li-ion battery would be a conservative choice. As a result of the inclusion of cathodic plies, SB feature a higher weight density than typical CFRP. Numerical values for the basic properties of the CFRP are compared to those adopted for SB in Table 3 in the example presented in Section 1.

Components made of composite materials like CFRP and SB can be reinforced with a core featuring specific characteristics. For aeronautical applications, besides the structural resistance and low weight, also flame resistance and limited change of these properties with respect to temperature are of interest. A family of materials which can be used for the composite core and bearing these characteristics is that of Nomex honeycomb. Composite panels or stringers filled with this core can be made thinner while keeping their resistance, and they are therefore more weight efficient.

The sizing of the structure components of the wing for each assigned option can been carried out considering an elliptical lift distribution over the wing span. The intensity of the lifting force is determined based on certification limits on the normal load factor. Safety factors can be similarly set according to the standard rules for certification. Stress limit criteria for composite materials can be safely applied also to the case of SB (Senokos et al. 2018). The result of the sizing process comes in terms of minimum area values for the stringers and the thickness of the panels capable of sustaining the imposed loads, while keeping within the limits imposed by certification constraints.

As a result of the structural computation, it is possible to evaluate the total volume of the wing structure and the corresponding weight. Considering all configurations, this computation will yield a different weight share of SB vs. standard structural components for each of them. This share can be applied at this level also to the fuselage and empennages, and in general to the weight of all components which can be manufactured in SB. This yields a total value of SB weight W_{sb}, and correspondingly a total weight of the conventional structure W_{cs} with no energy storage capability.

Finally, the weight W_{cb} of the conventional battery pack can be determined to meet the requirement of electric energy and power which is not assured by the SB. In analytic terms,

$$W_{\mathrm{cb}} = \max\left\{ \frac{E_{\mathrm{e}} - E_{\mathrm{sb}}}{e_{\mathrm{b}}}, \frac{P_{\mathrm{e}} - P_{\mathrm{sb}}}{p_{\mathrm{b}}} \right\}, \tag{2}$$

where P_{sb} and E_{sb} are the power made available and energy stored in the SB, and are proportional to the weight of the SB. More than one conventional battery technology can be considered, and that which is capable of minimizing the weight W_{cb} in Eq. 2 may be selected. Every conventional battery technology is associated to a corresponding value of e_{b} and p_{b}, which are therefore inherently bound to each other.

It shall be remarked that the optimal problem presented in Eq. 2 may produce unstable results over the iterations of the design loop displayed in Fig. 3. As a matter of fact, no such issues have shown up in practice, possibly as a result of the slight changes encountered by the quantities appearing in Eq. 2 over in the iterative design process.

When the weight of conventional structures and both the structural and conventional battery weights are known, the choice of the winning structural configuration can be carried out based on the selection of the lowest overall weight, *i.e.* the optimal design corresponds to the lowest value of the sum $(W_{\mathrm{cs}} + W_{\mathrm{sb}} + W_{\mathrm{cb}})$.

Empty weight estimation

In order to compute the overall take-off weight W_{to} corresponding to the optimal configuration, it is necessary to know the residual weight W_{ns} of the non-structural components of the airframe, usually accounted for in the empty weight – e.g. power plant, on-board systems, landing gear, etc. The overall empty weight W'_{e}, taking into account also the weight of the structure and propulsion system for standard aircraft with no SB, is typically bound to W_{to} by means of a statistical regression valid for an assigned aircraft category – *i.e.* aircraft with a similar mission and weight. This comes in the usual logarithmic form proposed by Roskam, $\log(W'_{\mathrm{e}}) = A + B\log(W_{\mathrm{to}})$ (Roskam 2003).

Clearly, this computation leads directly to an estimate of W'_{e} from a guess of W_{to}. The weight of the structure of a standard aircraft without SB needs to be separated from the rest of the empty weight. In other words, the empty weight W'_{e} can be decomposed into

$$W'_{\mathrm{e}} = W_{\mathrm{ns}} + W_{\mathrm{ss}}. \tag{3}$$

where W_{ss} is the weight of the structure in a standard design with no SB (Roskam 2003).

To the aim of updating the maximum take-off weight of the aircraft as required by the design procedure, a statistical regression of the weight of the structure in a standard design W_{ss} with respect to the empty weight W'_{e} was derived. The regression data have been obtained from the structural weight of existing GA aircraft. The structural weight for aircraft in a class may be gathered from data by Roskam (Appendix A, part V (Roskam 2003)). Alternatively, class II estimation rules proposed by Roskam can be adopted to provide an estimation of the structural weight of the different parts of the structure of more recent GA aircraft, drawing a value for W_{ss} based on its components.

Once built up, this regressive law allows to estimate W_{ss} from the value of W'_{e}. This in turn allows to compute W_{ns} from Eq. 3.

Updating the take-off weight and closing the weight sizing loop

Once the value of all components of the take-off weight has been guessed, it is possible to update its value, adding also the payload component W_{pl} based on the definition in Equation 1. Consequently, also the reference surface S_{ref} will be updated to a new value, based on the selected wing loading $W_{\mathrm{to}}/S_{\mathrm{ref}}$.

The procedure can be stopped based on an analysis of the evolution of W_{to}. The exit condition for the loop shall be set so that a minimum change of W_{to}, such as 1%, is necessary to continue running the cycle.

Based on experiments with several initial guesses, structural configurations, and SMP constraints, it can be said that the procedure is stable and converges to a solution when all parameters are set to values with a reasonable physical meaning. On the other hand, as a result of extreme values of the parameters, the solution may converge to unrealistic weight solutions. This is not dissimilar though from the outcome of most automatable preliminary design procedures for standard aircraft, hence not inherent to the use of SB.

DETAILED STRUCTURAL SIZING

Among the weight components in Eq. 1, the weight of the structure W_{cs} and of the SB W_{sb} should be met by means of a dedicated structural design procedure. An illustration of the proposed design procedure is presented in Figure 4. Besides the geometrical constraints and a desired weight of SB ensuing from the preliminary sizing, a desired range for the longitudinal positioning of the center of gravity is also imposed for stability. The whole sizing procedure is iterated based on the satisfaction of the latter.

A complete stick model of the aircraft is assembled based on the weight distribution and aerodynamic characteristics from the preliminary design (Szabo and Babuska 1991), and subjected to a full array of design load cases as prescribed by CS 23 (Various Authors 2015). The loads on the most stressed components of the

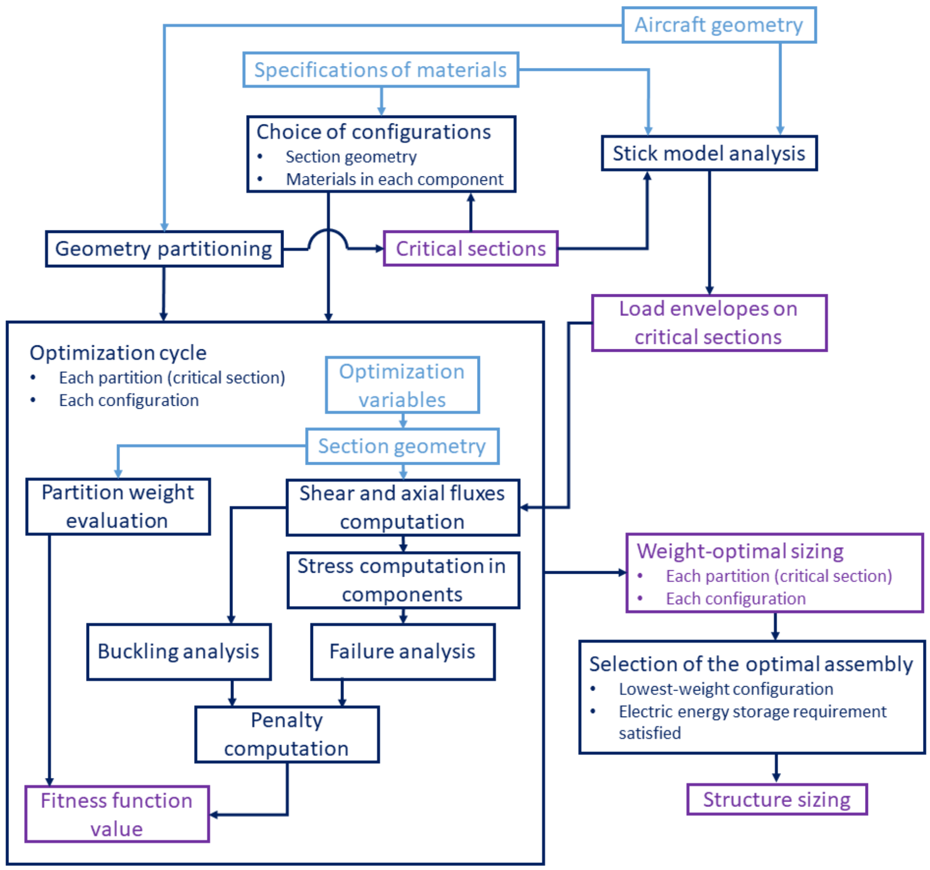

FIG. 4. Structural sizing flowchart.

structure are evaluated, including shear, bending and torsional moments, providing the input for the sizing process of the sections. In order to achieve good accuracy in the computation of loads, for the aero-elastic response of the aircraft in this phase it is possible to adopt a description of the CFRP (not of the SB) based on the model of ` black aluminium', *i.e.* an isotropic material with weight and stiffness properties mostly resembling those of the original composite material. This material is used for the fuselage, wing and tail, which will be manufactured in composite materials, either CFRP or SB.

The design of the structure is based on dividing the entire aircraft into partitions. In particular, for a GA aircraft it can be assumed that the half-wing and fuselage are divided into three partitions each, and the horizontal and vertical tail account for one partition each. The choice of the number of partitions is the result of a trade-off between the accuracy of the structural description and the computational cost. The characteristic section of each partition is modeled based on the usual semi-monocoque beam theory.

Structural arrangement of specific sections

Before proceeding with the sizing of the critical sections, the proposed procedure calls for a preliminary description of the main characteristic of the typical section of each partition of the structure. Assuming the partitioning of the aircraft structure presented above, typical of a GA aircraft, the layout of the fuselage and wing section needs to be specified.

The fuselage of modern GA aircraft is typically made of composite sandwich, easing the structural design and the manufacturing process thanks to the removal of all frames (Botelho et al. 2006). When SB are considered in the design, they can be placed also in the fuselage. This was already taken into account in the preliminary weight sizing. A core layer can be included between the carbon fiber layers to increase buckling critical loads. For this type of aircraft the fuselage section typically features a regular curvature – circular or oval – and can be modeled based on a proper number of panels according to the monocoque model. If structurally significant, the cabin floor can be modeled as a single additional panel made of CFRP sandwich with a reinforcing core, jointed with hinges to the external section, thus only transferring inertial forces due to the weight of the part of the on-board equipment anchored to the floor of the aircraft.

At the adopted level of detail, the presence of openings and doors in the composite structure can be taken into account by imposing a weight penalty on the overall structure. This is representative of the presence of reinforcements as required by discontinuities in the structure.

The structure of the wing can be considered as composed of a single cell box featuring a front and a rear spar. Both the panels and reinforcing stringers can be made of composite material, either standard CFRP or SB. Concerning SB, the existing specimens have been assembled as standard laminates. Besides this technological solution, a sandwich constructions with SB and a Nomex honeycomb filler has been envisaged in the present work, to increase bending stiffness of SB panels, so as to improve buckling characteristics. Nomex honeycomb can be used as a filler also for the stringers, to increase the shear-supporting area without dramatically increasing weight, and to have better flame resistance performance. Ω-shaped stringers are typically adopted for this type of structure on smaller aircraft, as they are especially suited for filling thanks to their shape. Due to its critical function on aerodynamic performance, the leading edge of the wing profile will be manufactured in a composite sandwich with a core layer, thus increasing its stiffness. As usual for classic wing structures, ribs can be modeled as plates loaded on the edges, being responsible for transferring shear loads due to the spanwise aerodynamic force distribution to the wing box.

The same sectional layout of the wing is adopted also for the horizontal and vertical stabilizers. All control surfaces are made of CFRP and not of SB, in consideration of potential difficulties in linking these parts to the on-board electrical plant, especially due to their small size hampering accessibility and internal allowances.

Optimal sizing of the critical sections

Partitions in the fuselage, wing and tail are sized independently to the aim of minimizing the weight of the corresponding parts of the airframe, following an optimal approach. The variables of the optimization process are different for each considered major part of the airframe (fuselage, wings, empennages), on account of the specific shape of the corresponding section. Clearly, the variables reflect the materials chosen for manufacturing each of those parts. As shown on the scheme in Figure 4, the choice of materials is not made inside the optimization loop. Therefore, for each part of the airframe, several different optimization problems are solved, based on as many corresponding choices of the materials for the structural components (panels, stringers,...) considered in the characteristic section of that airframe part.

The optimization variables corresponding to the different types of partitions considered are specified in the following. For the fuselage partitions, the considered variables defining the geometry are the number of plies used in the upper, lower and lateral composite panels respectively, plus the thickness of the sandwich core. This yields 12 variables when optimizing together the three fuselage partitions.

For the wing partitions, the optimization variables are the number of plies in the upper and lower panels and stringers respectively (2 variables), the number, thickness and sectional area of upper and lower stringers respectively (6 variables), the number of plies and the width of the spar webs, the number of plies in the spar caps, the number of ribs and of the plies in each rib. The total number of variables for each wing partition totals 13, yielding 39 optimization variables for a three-partitioned wing.

In order to reduce the size of the problem, some *a priori* constraints are imposed to the structure, resulting in a lighter numerical optimization process. The number of plies in the panels and stringers of the wing box can be set equal for the upper and lower components respectively, on account of a common practice allowing to reduce local stresses in the junction between these components. The sections of upper and lower wing stringers can be set equal, which may imply a reduced production complexity without a great loss of generality of the sectional model. Furthermore, by assuming that some structural components of the wing are uninterrupted, it can be that the width of the spar caps does not vary, whilst the number of stringers and the number of plies in the panels and spars does not increase from the root to the tip of the wing. This lowers the number of variables for the optimization of the wing to 18.

Concerning the choice of materials, several combinations are considered for each part of the airframe.

	Configuration	Panels	Floor
1	All CFRP	CFRP	CFRP
2	SB floor, CFRP	CFRP	SB
3	CFRP floor, SB	SB	CFRP
4	All SB	SB	SB

TABLE 5. Considered configurations of materials in fuselage.

	Configuration	Leading edge	Lower panels	Ribs	Spars
1	All CFRP	CFRP	CFRP	CFRP	CFRP
2	SB l.e., CFRP	SB	CFRP	CFRP	CFRP
3	SB lower panels, CFRP	CFRP	SB	CFRP	CFRP
4	SB lower panels + l.e., CFRP	SB	SB	CFRP	CFRP
5	SB l.e. + ribs, CFRP	SB	CFRP	SB	CFRP
6	SB spars + ribs, CFRP	CFRP	CFRP	SB	SB
7	SB spars, CFRP	CFRP	CFRP	CFRP	SB
8	All SB	SB	SB	SB	SB

TABLE 6. Considered configurations of materials in wings.

These are listed in Tables 5 and 6. For the fuselage partitions, four options are assumed, where the structure is completely made of CFRP, all except the floor which is manufactured in SB, a third configuration which is the dual of the latter where all the structure is manufactured in SB except the floor in CFRP, and finally one where the whole structure is made of SB.

For the wing partitions, again the extreme configurations are a structure made respectively of CFRP (number 1) or SB only (number 8). Other six options have been considered, featuring a different share of SB over CFRP. A first (number 2) with all the wing made of CFRP, except the leading edge, made of SB. Other two (numbers 3 and 4) are based on the lower panels and stringers made of SB. Lower panels are usually not compressed in flight, and recalling the relatively poor characteristics of this material under compression forces, this explains this configuration. The first of these two configurations features the leading edge made of SB too, the other the leading edge made of CFRP. The remaining three configurations (numbers 5 to 7) are conceived to test the advantage of adopting SB in the innermost structural components. In the first one, the leading edge and ribs are made of SB, in the second the whole wing is made of SB except the spars and ribs, made of CFRP as usual, and in the third one only the spars are made of SB.

Tail partitions are analyzed under configurations similar to the wing, but recalling that the horizontal and vertical empennages account for one partition each, they are lighter to treat from a numerical point of view.

The weight minimization process on each part of the airframe has to be constrained in order to guarantee the satisfaction of failure criteria on the corresponding structural component. In an optimization step, the current values of the optimization parameters produce a complete sectional topology and size. With the assigned selection of materials for each component of the sections, it is possible to compute the stress acting on that component, based on the usual semi-monocoque model. Failure of the composite laminates can be first checked with respect to the Tsai-Hill criterion (Hill 1950; Tsai and Wu 1971). Wing panels and ribs can be checked for buckling (Lekhnitskii 1968), whereas composite stringers can be checked for both crippling (Needham method) and Euler buckling (Bruhn 1973). Further failure criteria may include those for wrinkling and crimpling on the composite sandwich panels (Allen 1969). For the fuselage, buckling instability criteria for composite cylinders under compression, torsion and bending loads can be applied (Wang and Santo 1953).

The weight of the partitions in the fuselage wing and tail is minimized independently from the partitions in another part of the airframe. The optimization can be carried out through a genetic algorithm. This generally more computationally expensive method is needed due to the potentially poorly convexity of the merit function with respect to the parameters, leading to a potentially high number of local minima. In this scenario, the direct application of the failure criteria as constraints would lead to a very irregular behavior of the space of feasible solutions, thus further slowing convergence to a global optimum. An unconstrained optimization with a penalty method is more suited in this scenario. With this approach the weight of the structure is artificially increased, with a penalty computed based on the severity of the failure of the components in the partition, analyzed under the criteria mentioned above. Clearly, this approach will bear a optimum not necessarily compliant with the failure criteria. Therefore, after reaching an optimal configuration, a final check of the solution with respect to the failure criteria will be necessary.

Once the weight of all the airframe parts have been optimized for all considered combinations of structural materials, it is possible to complete the structural design by assembling the optimal solutions for each airframe part in such a way to obtain the minimum overall weight of the structure with a share of structural battery sufficient to comply with the weight requirement coming from the preliminary weight sizing.

The detailed design of the structure enables a precise estimation of the center of gravity (CG), provided all other weights have been localized with respect to the geometry – something which is required at the level of the synthesis of the stick model to accurately account for inertial loads. The positioning of the CG may be checked with respect to maneuverability and controllability criteria. In case the resulting qualities are not satisfactory, the geometry and weight positioning may be altered, thus triggering a further structural design loop.

If, at the end of the optimization, no solution exists capable of satisfying the requirement on SB weight, or the advantage with respect to a configuration with no SB is negligible, this may indicate the performance of the adopted materials, including SB, is too poor for the required mission specifications.

HYBRIS CASE STUDY

An application of the proposed procedures for the preliminary weight sizing and structural sizing of a light aircraft with SB is represented by the award-winning design project *Hybris* (Bernasconi et al. 2017). The project ranked first in the open competition launched by the Royal Aeronautical Society in 2016 to the aim of promoting brand-new ideas towards the renewal of the aging GA fleet, especially in the United Kingdom.

The requirements for this aircraft were set according to the results of interviews with a wide variety of potential customers, both private owners or flight schools and aero clubs. Looking at the degree of satisfaction with respect to the aircraft models currently in the GA fleet in terms of flight performance, operation and maintenance costs, as well as other features, the adopted configuration is that of a four-seater with a low wing and a usual tricycle retractable landing gear. The serial hybrid-electric propulsion system features a single tractor propeller. Figure 5 shows the outer appearance of the Hybris.

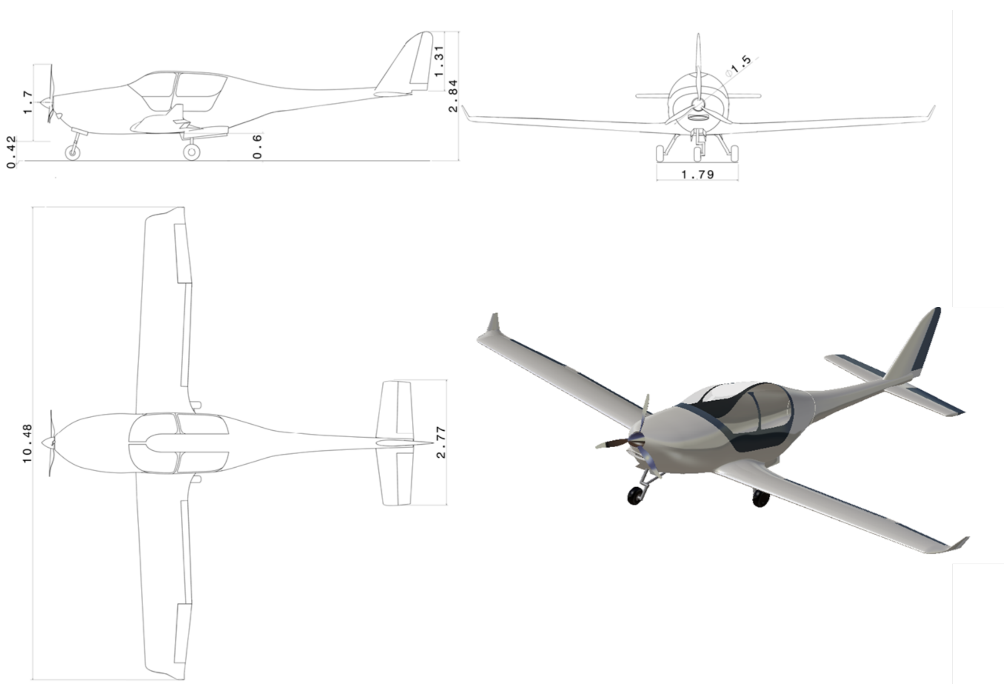

FIG. 5. Hybris three-view with rendering (all values in meters).

Preliminary weight sizing

The desired performance and design flight profile emerging from the preliminary study are presented in Table 8 and Figure 6, respectively. The proposed flight profiles are a traditional cross-country mission, and a training mission as well. The ceiling and cruising altitude are not very high for the category, on account of the relatively low peaks in the orography of the United Kingdom. The propulsion system is serial hybrid-electric, where a single main ICE installed in the back of the cabin is used to provide electric power to drive the EM and/or recharge the batteries. The power management profile features terminal maneuvers in all-electric mode. Above 3,000 ft the ICE is switched on, whereas it is not used otherwise, to save on noise and pollutant emissions around departure and destination airfields and while flying close to the ground.

Requirement	Value
V_{st}	31.4 m/s
L_{to}	450 m
L_{lnd}	400 m
V_v	5.2 m/s
$V_{v_{\mathrm{OEI}}}$	0.84 m/s
V_{cruise}	77 m/s

TABLE 7. Hybris performance requirements for the sizing matrix plot.

Requirement	Value
R_{cr}	925 km
V_{cr}	77 m/s
h_{cr}	2 440 m
h_{ceil}	3 000 – 4 500 m
Occupants	3 + pilot

TABLE 8. Hybris main mission requirements.

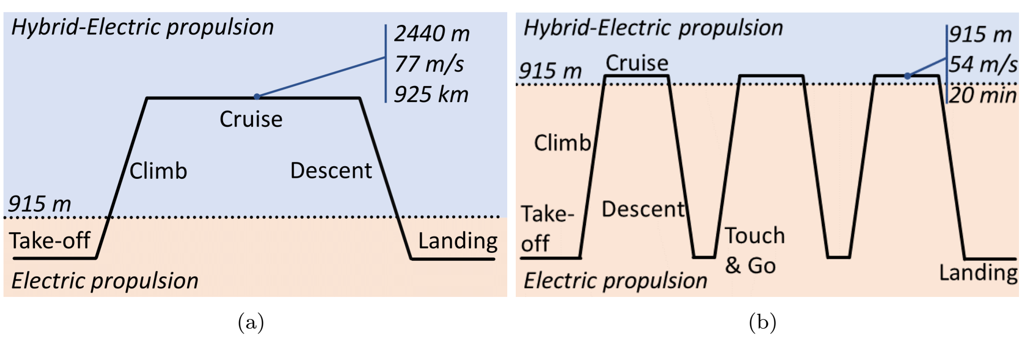

FIG. 6. Hybris design flight profile. (a) Cross-country mission. (b) Training mission.

As mentioned above, the preliminary weight sizing can be carried out starting from the SMP of the aircraft. Pertinent regulations are EASA CS 23. Take-off and landing distances, stall speed and climb rate of competing aircraft already in use have been taken into account in the formulation of the SMP constraints.

Table 7 highlights the considered performance minima to be satisfied. The resulting SMP is presented in Figure 7, where the performance curves account for a polar of the aircraft which has been computed based on the procedures by Roskam (Roskam 2003) for the assumed configuration and level of technology. The corresponding values are seen in Table 9. It is noteworthy that a value of aspect ratio λ needs to be guessed at this level. Once also the reference wing area S_{ref} is assigned, these lead to specific values for wing span and mean aerodynamic chord length. Looking at Figure 7, the requirements bound to the cross-country mission profile turned out to be more stringent than those from the training profile (Figure 6). Furthermore, for a preliminary analysis, also the OEI climb requirement has been accounted for, so as to keep a multi-engine configuration among the possible design solutions.

Configuration	Clean	Take–off	Landing
C_{D_0}	0.02	0.026	0.026
$C_{L,\max}$	1.4	1.6	1.9
e	0.85		
λ	9.0		

TABLE 9. Hybris guessed polar coefficients.

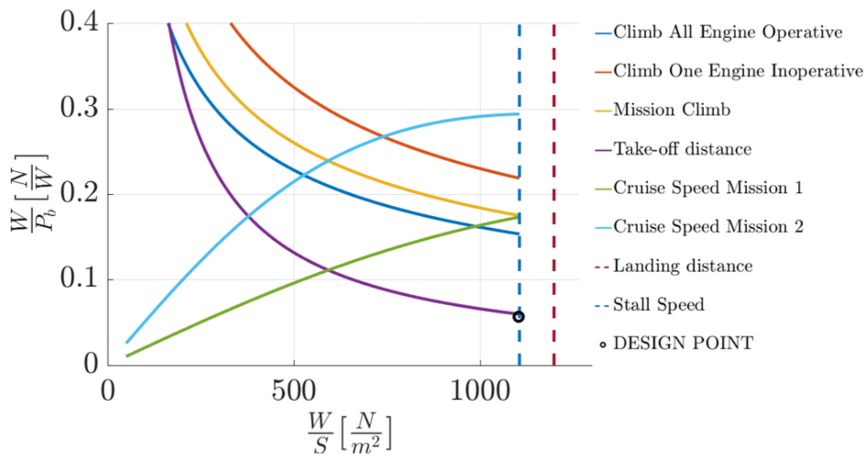

FIG. 7. Hybris sizing matrix plot.

The selected design point allows to minimize required power and surface for an assigned weight. The choice of a point further left on the plot, corresponding to a larger wing area and correspondingly more SB, was discarded in favor of a more conservative design. This was due to the uncertainties related to SB technology in terms of energy storage efficiency, which might translate into too high a SB weight, when used to assemble a larger wing.

The coefficients A and B of the regression $\log(W_{\mathrm{e}}^{\prime}) = A + B\log(W_{\mathrm{to}})$ can be computed based on the data of the already flying competitors.

Concerning the structure, at this level a single cell was considered and analyzed using a method proposed by Gudmundsson (Gudmundsson 2013), adjusted for this application. The spar and the panels were verified with respect to CS 23 stress limits. SB were treated as composites from a structural modeling viewpoint, as proposed by Wetzel (Wong et al. 2007).

Seven wing configurations were analyzed at this stage with different choices of materials (listed in Table 4 and described in Section 3). It is remarked that, due to the generally poor behavior of SB under compression, this material was not used in the upper panels and stringers.

As previously explained, the computation of the weight of the conventional batteries can be performed when the weight of the SB is known, *i.e.* following the computation of the weight of the structure for a guessed configuration of the materials. To allow using Eq. 2, it is necessary to know the energy and power density of conventional batteries. In order to obtain the minimum possible weight of the battery, many battery types have been considered, each with an energy density e_{b} and a power density p_{b}.

The energy and power needed come from the assigned mission profile and power management profile. Power and energy losses in the cables and ancillary systems have been considered adding a 5% increase on required power and a 25% increase on required energy.

The technology yielding the minimum W_{cb} from Eq. 2 was be selected. The corresponding values of energy and power density for both SB and conventional batteries are reported in Table 2.

Following the sizing methodology previously described and presented in Figure 3, after some iterations convergence is obtained. Table 10 lists the resulting weight, geometry and power characteristics of the considered design point.

Specifications	Value
W_{cb}	35 $\mathrm{kg_f}$
W_{sb}	109 $\mathrm{kg_f}$
W_{cs}	129 $\mathrm{kg_f}$
W_{ns}	611 $\mathrm{kg_f}$
W_{f}	76 $\mathrm{kg_f}$
W_{pl}	300 $\mathrm{kg_f}$
W_{to}	1 260 $\mathrm{kg_f}$
P_{b}	218 kW
S_{ref}	11.2 m^2

TABLE 10. Hybris design weight breakdown.

Structural sizing

The design of the structure was carried out in accordance with the procedure presented above. The composite materials considered are CFRP and SB using Poly-Acrylo-Nitrile (PAN) carbon fibers, which feature better Li-ion storage capabilities, at the cost of a tensile strength lower than other carbon fibers commonly employed on airframes. Table 3 lists the basic characteristics of the composite materials considered for this design.

As previously highlighted, a material typically used as a core in sandwich composites is the Nomex honeycomb. The properties of HexWeb HRH10-4.8-96 have been used in structural computations.

The stick model of the aircraft was assembled in `Nastran`. The external sizing was determined based on the aerodynamic design of the aircraft, documented in (Bernasconi et al. 2017), whereas the thickness of the sections was set in order to comply with the weight computations completed in the preliminary design phase. The material used in this phase is black aluminium, an isotropic material bearing structural characteristics comparable to those of the adopted composites (Liu et al. 2009; Snyder et al. 2007). The stick model was subjected to the conditions prescribed by EASA CS 23 (book 1 part C).

The load envelopes determined using the stick model were used to size the critical sections. As shown in Fig. 8, the fuselage and each half wing was modeled in three partitions, the horizontal and vertical tail assemblies accounted for one partition each. The materials configurations already introduced were considered for the critical sections.

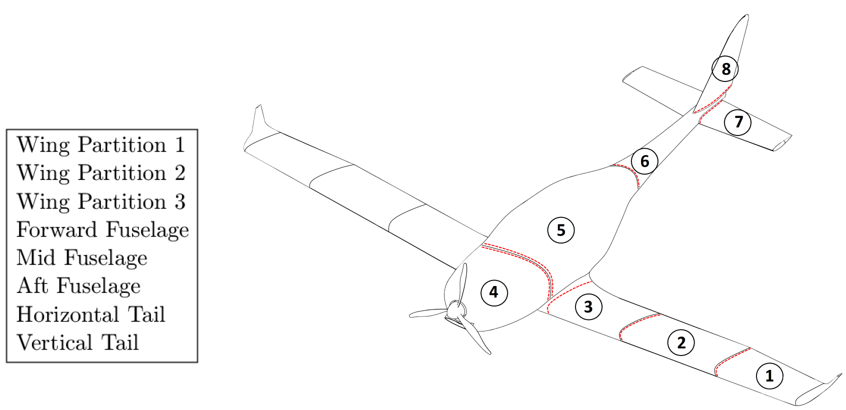

FIG. 8. Partitions of wing, fuselage and empennages.

The independent optimization of the main parts of the airframe led to the results in Tables 11, 12, and 13. The optimization was carried using the genetic algorithm in the *Global Optimization Tool* of `Matlab`. Figure 9

526 shows the corresponding Nastran structural and aerodynamic models (the latter based on the code built-in
527 vortex-lattice method).

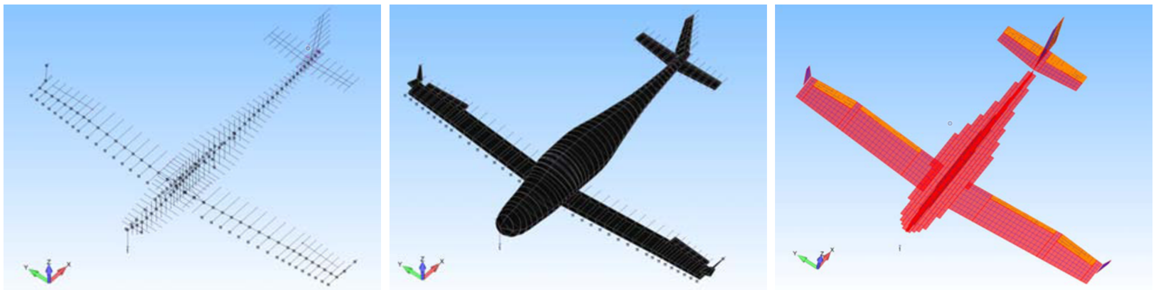

(a) (b) (c)

FIG. 9. Hybris Nastran modelling. (a) Beams and masses. (b) Beams with cross sections. (c) Aerodynamic lattice.

Fuselage partition	Configuration	Total [kg_f]	SB [kg_f]
1	All CFRP	71.03	0.00
2	SB floor, CFRP	78.58	9.77
3	CFRP floor, SB	92.68	61.25
4	All SB	100.23	75.91

TABLE 11. Hybris optimal structural weight results for the fuselage, with different configurations of materials.

Wing partition	Configuration	Total [kg_f]	SB [kg_f]
1	All CFRP	111.50	0.00
2	SB leading edge, CFRP	114.47	8.40
3	SB lower panels, CFRP	121.97	39.07
4	SB lower panels + leading edge, CFRP	124.94	47.47

TABLE 12. Hybris optimal wing structural weight results with different material configurations.

Empennage	Total [kg_f]	SB [kg_f]
Horizontal tail	12.33	0.00
Vertical tail	7.87	0.00

TABLE 13. Hybris optimal empennage structural weight results with different material configurations.

528 According to the scheme in Figure 3, the final combination of Tables 11, 12, and 13 was selected in order to
529 obtain the minimum structural weight while assuring the required weight of SB. The configurations featuring
530 a lower use of SB were analyzed first. More configurations were studied until the minimum weight of SB from
531 the preliminary design was obtained.

Considering the wing, by proceeding in the analysis of the configurations in the order proposed in Table 12, when a satisfactory combination was found the analysis was stopped. Indeed, a higher share of components made of SB would raise their weight above the design target obtained from preliminary weight sizing. For this reason, comparing the cases reported introduced in Table 6 and those reported in Table 12, it can be noted that several configurations for the wing and empennages were not actually studied.

As seen in Table 13, the empennages were considered to be entirely made of CFRP, avoiding to consider combined CFRP and SB, for the sake of simplicity and on account of their relative small size and corresponding contribution to energy storage. Also, having reached the target weight for SB by adopting them for the fuselage and parts of the wing, their use in the tail was not needed.

The final optimal solution is presented in Table 14.

Part	Configuration
Fuselage	CFRP floor, SB
Wing	SB lower panels + leading edge, CFRP
HT	CFRP
VT	CFRP

TABLE 14. Hybris optimal structural design configuration.

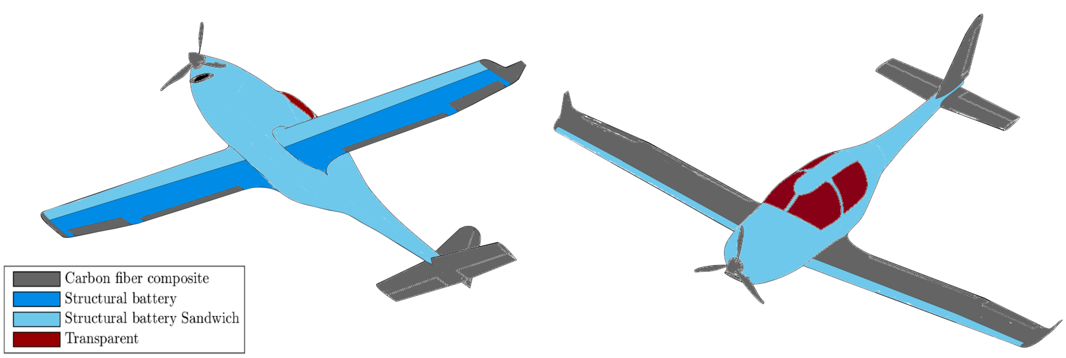

FIG. 10. Use of materials in the Hybris airframe.

A sketch of the adopted configuration of materials is presented in Figure 10. While apparent that CFRP has been adopted for all the empennages, it is also noteworthy that the the fuselage is mostly made of SB, with the floor panel (not visible from the sketch in Figure 10) made of CFRP as specified in Table 14. The lower panels of the wing are made of SB, whereas as from Table 14 the rest of the wing structure is made of CFRP. Figure 11 shows a typical wing section. This is an exemplar outcome of the optimization process, where the number of stringers as well as the thickness of panels and areas of the stringers are computed

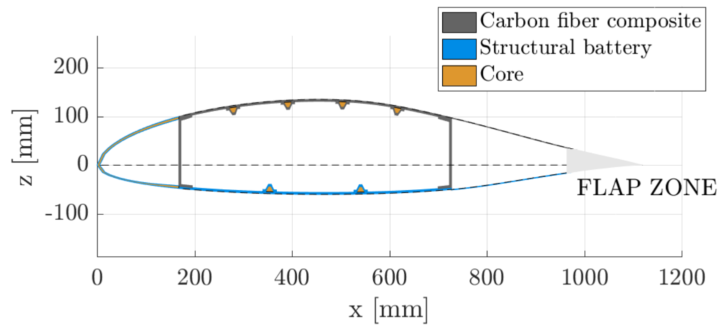

FIG. 11. Wing root section in the Hybris optimal configuration.

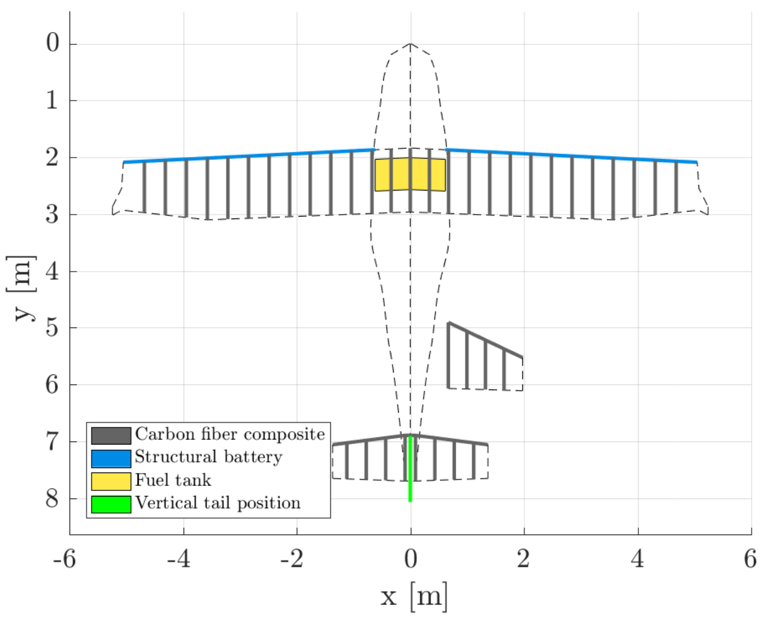

FIG. 12. Rib arrangement in the Hybris optimal configuration.

to sustain all design load cases, while at the same time assuring minimum weight, taking into account the materials adopted for each component. Similarly, Figure 12 shows the arrangement of the ribs resulting from the optimization, both for the wings and the empennages.

Table 15 shows the final results concerning the total weight of SB, the total weight of the airframe structure, and the design maximum take-off weight for the Hybris. Of the total structural weight, 45% is made of SB, while the rest consists in conventional CFRP.

Weight	Value [kg_f]	Fraction of W_{to}
SB weight	109	8.6 %
Total structure weight	238	18.9 %
Design take-off weight	1,265	100.0 %

TABLE 15. Hybris optimal structural design configuration.

Considering two candidate designs with the same MTOW, one using classic Al-alloy for the airframe and the other traditional composites, weight savings of 61.2 kg and 18.9 kg, respectively, are achieved. This translates in a percentage savings of 17.8% and 5.9%, respectively, compared to the weight of battery and structure, and of 5.1% and 1.5% with respect to MTOW. It should be remarked that this figure is due to the very conservative assumptions made on the actual technology level of SB, *i.e.* the 0.5 safety factor imposed on energy density figures with respect to evolution projections based on data found in literature (Asp and Greenhalgh 2014; Ekstedt et al. 2010).

CONCLUSION

A novel procedure for the sizing of an aircraft employing the innovative technology of structural batteries (SB) in its airframe has been introduced. SB are a promising technology allowing to store electric energy while being capable of sustaining significant loads. The chance to laminate SB in curved panels and small-section stringers allows to deploy this material in key areas of the aircraft structure, today manufactured in conventional composite materials. To the authors' knowledge, this is the first attempt to consider SB in the structural design of an airplane, providing a methology to determine its preliminary weight sizing and its structural configuration and sizing.

The proposed sizing methodology features two major stages. In the preliminary weight sizing stage, the weight of structural batteries necessary to sustain certification loads is computed together with all other major weight components in an iterative fashion, based on some assumptions concerning the adoption of a share of SB in a series of considered structure configurations. Thanks to the adopted sizing criteria, the battery weight – including a significant share of SB – obtained from this computation is such to satisfy energy and power requirements from the mission profile. These may reflect the choice of a all-electric or hybrid-electric power source, thus yielding a potentially broader applicability of the considered procedure with respect to the design example presented herein.

The weight of SB from this stage represents a target value for the second stage of the sizing procedure. Here the structure of the section of the fuselage, wing and empennages, suitably partitioned to take into account non-uniform structural characteristics along their respective lengths, is optimized considering a number of geometric parameters. These include the thickness of the panels, areas of stringers, and their corresponding number. Multiple optimization runs are performed on the section of each main part of the airframe, each based on a hypothesized construction material for the components of the section. The optimization targets the overall weight, with constraints to assure the satisfaction of structural integrity criteria.

It may be remarked that the procedure bends itself to a looping algorithm, where the final weight configuration can be used to update the preliminary estimation of the weight components (especially the empty weight), as usual in aircraft design procedures for more conventional structural configurations.

A realistic application of the proposed procedure has been presented through the results of the award-winning project *Hybris*, a GA aircraft with serial hybrid-electric propulsion. The results demonstrate the applicability and functionality of the procedure in both the stages envisaged, which yield realistic results in line with typical weight values and structure configurations of today's aircraft with comparable weight and mission. Compared to a design where SB are not considered, the modest weight advantage provided by the adoption of SB instead of conventional CFRP obtained in the presented case is the result of a very conservative approach, where significant safety margins are assumed on the performance of SB, which are today still in an experimental stage. It is expected that when a better performance of SB would be safely assumed, the results will show a substantial improvement over a conventional composite design.

Naturally, the possible introduction of SB in airframes shall pose further important problems, such as those related to safety, on-board integration, maintenance, and cost. This is clearly beyond the scope of the present work, which may prove helpful in order to assess the general feasibility and possible advantages of SB adoption in aeronautics, justifying further studies, once significant improvements, especially in terms of environmental sustainability, are predicted.

FUNDING SOURCES

The Authors have not received any specific grant from any funding agency in the public, commercial, or not-for-profit sectors for the production of this research.

ACKNOWLEDGEMENTS

The contribution of A. Bernasconi, L. Capoferri, A. Favier, C. Velarde Lopez de Ayala, F. Gualdoni of the Department of Aerospace Science and Technology, Politecnico di Milano in the obtainment of the results is gratefully acknowledged. The insight provided by E.D. Wetzel, Ph.D., of the U.S. Army Research Laboratory on the technology of structural batteries has been instrumental in the design of the proposed procedure and in analyzing results in the considered test case.

DATA AVAILABILITY

All data produced and used in the presented case study are available from the corresponding author by request (not included herein for obvious reasons of length limitations).

Nomenclature

CFRP	Carbon Fiber Reinforced Polymer
GA	General Aviation
HC	Hydro-Carbon
HT	Horizontal Tail
ICE	Internal Combustion Engine
LSA	Light Sport Aircraft
SB	Structural Batteries
SMP	Sizing Matrix Plot
VT	Vertical Tail

REFERENCES

Adam, T. J., Liao, G., Petersen, J., Geier, S., Finke, B., Wierach, P., Kwade, A., and Wiedemann, M. (2018). "Multifunctional composites for future energy storage in aerospace structures." *Energies*, 11.

Allen, H. G. (1969). *Analysis and Design of Structural Sandwich Panels*. Pergamon Press.

Ampaire Inc. "3507 Jack Northrop Ave., Hawthorne, CA 90250, USA. www.ampaire.com.

Asp, L. E. (2013). "Multifunctional composite materials for energy storage in structural load paths." *Plastic, Rubber and Composites*, 42, 144–149.

Asp, L. E. and Greenhalgh, E. S. (2014). "Structural power composites." *Composites Science and Technology*, 101, 41–61.

Bernasconi, A., Biondani, F., Capoferri, L., Favier, A., Velarde Lopez de Ayala, C., Riboldi, C. E. D., and Trainelli, L. (September 18-22, 2017). "Conceptual design of a structural-battery hybrid-electric aircraft." *Proceedings of the 24th Conference of the Italian Association of Aeronautics and Astronautics (AIDAA 2017)*, Palermo-Enna, Italy.

Bona, G. E., Bucari, M., Castagnoli, A., and Trainelli, L. (June 16–20, 2014). "Flybrid: Envisaging the future hybrid-powered regional aviation." *Proceedings of the AIAA/3AF Aircraft Noise and Emissions Reduction Symposium*, Atlanta, GA.

Botelho, E. C., Silva, R. A., Pardini, L. C., and Rezende, M. C. (2006). "A review on the development and properties of continuous fiber/epoxy/aluminum hybrid composites for aircraft structures." *Materials Research*, 9, 3.

Bruhn, E. F. (1973). *Analysis and Design of Flight Vehicle Structures*. Jacobs Pub.

Cao, W., Mecrow, B. C., Atkinson, G. J., Bennett, J. W., and Atkinson, D. J. (2012). "Overview of electric motor technologies used for more electric aircraft (mea)." *IEEE Transaction on Industrial Electronics*, 59, 3523–3531.

Carlstedt, D., Marklund, E., and Asp, L. E. (2019). "Effects of state of charge on elastic properties of 3d structural battery composites." *Composites Science and Technology*, 169, 26–33.

Cohen, J. P. and Coughlin, C. C. (2008). "Spatial hedonic models of airport noise; proximity and housing prices." *Journal of Regional Science*, 48, 859–878.

Diamond Aircraft Industries GmbH. "N. A. Otto-Strasse 5, 2700 Wiener Neustadt, Austria. www.diamondaircraft.com.

Ekstedt, S., Wysocki, M., and Asp, L. E. (2010). "Structural batteries made from fibre reinforced composites." *Plastic, Rubber and Composites*, 39, 148–150.

Friedrich, C. and Robertson, P. A. (2015). "Hybrid-electric propulsion for aircraft." *Journal of Aircraft*, 52, 176–189.

Gienger, E. B., Nguyen, P. A. T., Chin, W., Behler, K. D., Snyder, J. F., and Wetzel, E. D. (2015). "Microstructure and multifunctional properties of liquid + polymer bicomponent structural electrolytes: Epoxy gels and porous monoliths." *Journal of Applied Polymer Science*, 132, 42.

Gudmundsson, S. (2013). *General Aviation Aircraft Design*. Butterworth-Heinemann, first edition edition.

Hagen, M., Dörfler, S., Fanz, P., Berger, T., Speck, R., Tübke, J., Althues, H., Hoffmann, M. J., Scherr, C., and Kaskel, S. (2013). "Development and costs calculation of lithium –sulfur cells with high sulfur load and binder free electrodes." *Journal of Power Sources*, 224, 260–268.

Hagen, M., Hanselmann, D., Ahlbrecht, K., Maca, R., Gerber, D., and Tübke, J. (2015). "Lithium-sulfur cells: The gap between the state-of-the-art and the requirements for high energy battery cells." *Advanced Energy Materials*, 5.

Hill, R. (1950). *The Mathematical Theory of Plasticity*. Oxford University Press, Oxford, England.

Johannisson, W., Ihrner, N., Zenkert, D., Johansson, M., Carlstedt, D., Asp, L. E., and Sieland, F. (2018). "Multifunctional performance of a carbon fiber ud lamina electrode for structural batteries." *Composites Science and Technology*, 168, 81–87.

Lange Aviation GmbH. "Brüsseler Straße, 30 D–66482 Zweibrücken, Germany. www.lange-aviation.com.

Lekhnitskii, S. G. (1968). *Anisotropic Plates*. Gordon and Breach Science Publishers.

Liu, P., Sherman, E., and Jacobsen, A. (2009). "Design and fabrication of multifunctional structural batteries." *Journal of Power Sources*, 189.

Morrell, P. and Lu, C. (2000). "Aircraft noise social cost and charge mechanisms - a case study of amsterdam airport schiphol." *Transportation Research Part D*, 5, 305–320.

Ozawa, K. (2009). *Lithium Ion Rechargeable Batteries*. Wiley-VCH, first edition edition.

Pearson, C., Thwaite, C., and Russel, N. (August 9-12, 2004). "The use of small cell lithium-ion batteries for more satellite applications." *Proceedings of the 18th Annual AIAA/USU Conference on Small Satellites*, Logan, UT.

Pipistrel Vertical Solutions d.o.o. "Goriska Cesta 50a, SI–5270 Ajdovšcina, Slovenia. www.pipistrel.si.

Rao, N. S., Simha, T. G. A., Rao, K. P., and Kumar, G. V. V. R. (2015). "Structural batteries, carbon composites are becoming competitive and cost effective." *White Paper infosys.com*.

Raymer, D. P. (2012). *Aircraft Design: A Conceptual Approach*. AIAA Education Series, fifth edition edition.

Riboldi, C. E. D. (2018). "An optimal approach to the preliminary weight sizing of small hybrid-electric aircraft." *Aerospace Science and Technology*, 81, 14–31.

Riboldi, C. E. D. and Gualdoni, F. (2016). "An integrated approach to the preliminary weight sizing of small electric aircraft." *Aerospace Science and Technology*, 58, 134–149.

Riboldi, C. E. D., Gualdoni, F., and Trainelli, L. (2018). "Preliminary weight sizing of light pure-electric and hybrid-electric aircraft." *Transportation Research Procedia*, 29, 376–389.

Roskam, J. (2003). *Airplane Design (Part I-VII)*. DAR Corporation, second edition edition.

Rossi, N., Salucci, F., Riboldi, C. E. D., Rolando, A., and Trainelli, L. (October 23–25, 2018). "A general approach to the conceptual design of all-electric and hybrid-electric aircraft." *Proceedings of the Advanced Aircraft Efficiency in a Global Air Transport System Conference (AEGATS 2018)*, Toulouse, France.

Scholz, A. E., Hermanutz, A., and Hornung, M. (September 4–6, 2018). "Feasibility analysis and comparative assessment of structural power technology in all-electric composite aircraft." *Proceedings of the Deutscher Luft- und Raumfahrtkongress*, Friedrichshafen, Germany.

Senokos, E., Ou, Y., Torres, J. J., Sket, F., Gonzalez, C., Marcilla, R., and Vilatela, J. J. (2018). "Energy storage in structural composites by introducing cnt fiber/polymer electrolyte interleaves." *Nature Scientific Reports*, 3407.

Snyder, J. F., Carter, R. H., and Wetzel, E. D. (2007). "Electrochemical and mechanical behavior in mechanically robust solid polymer electrolytes for use in multifunctional structural batteries." *Chemistry of Materials*, 19(15), 3793–3801.

Snyder, J. F., O'Brien, D. J., and Wetzel, E. D. (2016). *Structural Batteries, Capacitors and Supercapacitors*, Vol. Handbook of Solid State Batteries. World Scientific Publishing Co.

Szabo, B. and Babuska, I. (1991). *Finite Elements Analysis*. Wiley, New York.

Trainelli, L., Comincini, D., Salucci, F., Rolando, A., and Riboldi, C. E. D. (September 9–12, 2019a). "Sizing and performance of hydrogen-driven airplanes." *Proceedings of the Italian Associations of Aeronautics and Astronautics (AIDAA) 25th International Conference*, Roma, Italy.

Trainelli, L. and Perkon, I. (February 6–7, 2019). "Mahepa - a milestone-setting project in hybrid-electric aircraft technology development." *Proceedings of the More Electric Aircraft Conference (MEA 2019)*, Toulouse, France.

Trainelli, L., Rossi, N., Salucci, F., Riboldi, C. E. D., and Rolando, A. (September 9–12, 2019b). "Preliminary sizing and energy management of serial hybrid-electric airplanes." *Proceedings of the Italian Associations of Aeronautics and Astronautics (AIDAA) 25th International Conference*, Roma, Italy.

Tsai, S. W. and Wu, E. M. (1971). "A general theory of strength for anisotropic materials." *Journal of Composite Materials*, 5, 58–80.

Various Authors (2015). *Certification Specifications and Acceptable Means of Compliance for Normal, Utility, Aerobatic and Commuter Category Aeroplanes CS-23 - Amendment 4*. European Aviation Safety Agency (EASA), Brussels, Belgium.

Wang, C. T. and Santo, D. F. D. (1953). *Buckling of Sandwich Cylinders under Axial Compression, Torsion, Bending, and Combined Loads*. New York University, College of Engineering, Research Division, New York.

Wetzel, E. D. (May 13, 2010). "Perspectives on multifunctional energy-storing structures." *Air Force Office for Scientific Research Multifunctional Materials for Defense Workshop*, Reston, VA.

Wong, E. L., Baechle, D. M., Xu, K., Carter, R. H., Snyder, J. F., and Wetzel, E. D. (June 3–7, 2007). "Design and processing of structural composite batteries." *Proceedings of the SAMPE 2007 Symposium*, Baltimore, MD.

Yuneec Americas (USA). "5555 Ontario Mills Parkway, Ontario, CA 91764, USA. www.yuneec.com.